PHYSICAL REVIEW B VOLUME 4, NUMBER 2 15 JULY 1971

Study of Room-Temperature Photomagnetoelectric and Photoconductive Effects in Au-Doped Silicon

S. S. Li and H. F. Tseng
Electrical Engineering Department, University of Florida, Gainesville, Florida 32601
(Received 6 January 1971)

Recombination properties of the photoinjected carriers in gold-doped n-type and p-type silicon have been investigated at $T=300\,°K$ using measurements of the steady-state photomagnetoelectric (PME) and photoconductive (PC) effects. A theory for the PME and PC effects in Au-doped silicon has been developed for the case of low injection and arbitrary trapping. The theory was checked by calculating the electron- and hole-capture probabilities at the gold acceptor and donor levels from the PME and PC measurements, using the ratios of the electron-hole capture rate given by Fairfield *et al.*, and the results are found to be in good agreement with those determined from other methods.

I. INTRODUCTION

In our recent study of the low-temperature photomagnetoelectric (PME) and photoconductivity (PC) effects in Au-doped silicon,[1,2] we reported that at very low temperatures (from 4.2 to 100 °K) a nonlinear quadratic relationship was obtained between Δp and Δn (i.e., $\Delta p=\Gamma\Delta n^2$) at moderate injection range as a result of the hole trapping at the gold-acceptor levels. This results in a $\frac{4}{3}$ power-law relation between PME short-circuit current and the PC (i.e., $I_{\text{PME}}\propto\Delta G^{4/3}$). In this paper, we report the results of room-temperature measurements of the PME and PC effects in a relatively thin Au-doped silicon ($d\simeq 0.1$ mm) sample. A method of determining the recombination parameters such as electron and hole lifetimes, the electron- and hole-capture probabilities at the gold levels using steady-state PME and PC effects is demonstrated in the present paper. The results are found to be in good agreement with the experimental data available in the literature as determined from the Hall effect, PC decay, and photovoltaic effect experiments.[3–5]

II. THEORY

The physical model used in developing the room-temperature recombination theory and the PME effect in Au-doped silicon is based on the following assumptions and facts: (i) The samples were overcompensated by gold impurity (i.e., $N_{\text{Au}}>N_D$ or $N_{\text{Au}}>N_A$), and thus in the exhaustion region, $N_{\text{Au}}\gg n_0$. (ii) Small injection ($\Delta n<n_0$, or $\Delta p<p_0$) and small magnetic field ($\mu B<1$) conditions are assumed. (iii) The generation of electron-hole pairs by incident photons is in the vicinity of the illuminated surface (i.e , $\alpha d\gg 1$), where α is the absorption coefficient and d is the sample thickness. (iv) The surface recombination velocity s_0 on the illuminated surface is much smaller than the dark surface recombination velocity s_d (i.e., $s_0\ll s_d$). (v) One-dimensional analysis is valid ($l\gg d$) and the end effect is ignored. The notations used above, unless otherwise specified, have the conventional meanings.[1]

A. Excess-Carrier Lifetimes and the Ratio of Excess-Carrier Density

In order to interpret the steady-state PME and PC effects in Au-doped silicon, it is necessary to develop the expressions for the excess-carrier lifetimes and the ratio of injected excess-carrier density. In the case of gold-overcompensated silicon, the Fermi level is locked near the center of the forbidden gap, and the gold concentration and the shallow donor (or acceptor) density will be much larger than the thermal-equilibrium concentration of the free carriers (i.e., N_{Au}, $N_D\gg n_0$, p_0 or N_{Au}, $N_A\gg n_0$, p_0). The recombination and trapping mechanism for such samples is that only one of the two levels of the gold atoms in the band gap will be effective in recombination process (i.e., acceptor level for n-type material, and donor level for p-type samples); the other level will act as a trapping center for minority carriers.

The density of gold atoms with different charge states can be expressed as follows:

(a) For n-type material,

$$N_{\text{Au}}^0=N_{\text{Au}}-(N_D-n_0)\simeq N_{\text{Au}}-N_D \qquad (1)$$

is the density for neutral gold centers, and

$$N_{\text{Au}}^-=N_D-n_0\approx N_D \qquad (2)$$

is the density for negatively charged gold-acceptor centers.

(b) For p-type material,

$$N_{Au}^{0} = N_{Au} - (N_A - p_0) \simeq N_{Au} - N_A \ , \tag{3}$$

and

$$N_{Au}^{+} = N_A - p_0 \approx N_A \tag{4}$$

is the density for positively charged gold-donor centers. For small injection case (i.e., $\Delta n \ll N_{Au}^0$, $\Delta p + \Delta p_t \ll N_{Au}^-$, N_{Au}^0 for n type; $\Delta p \ll N_{Au}^0$, $\Delta n + \Delta n_t \ll N_{Au}^0$, N_{Au}^+ for p type), the variation of gold charge states with injection can be ignored. Therefore, the lifetimes of the injected carriers are independent of the light intensity.

For n-type samples, the electron lifetime τ_n (τ_n is defined as the free time that an electron spends in the conduction band before being captured by the neutral gold-acceptor level) can be expressed by

$$\tau_n = \frac{1}{C_n^0 N_{Au}^0} = \frac{1}{C_n^0 (N_{Au} - N_D)} \ , \tag{5}$$

where C_n^0 is the rate of electron capture probabilities ($cm^3 \, sec^{-1}$) by the neutral gold-acceptor centers, and N_{Au}^0 is substituted by $(N_{Au} - N_D)$ using Eq. (1). The hole lifetime τ_p at the negatively charged gold-acceptor centers can be expressed by

$$\tau_p = \frac{1}{C_p^- N_{Au}^-} = \frac{1}{C_p^- N_D} \ , \tag{6}$$

where C_p^- represents the rate of hole-capture probabilities by the negatively charged gold-acceptor centers, and N_{Au}^- is substituted by N_D using Eq. (2).

Similarly, the electron and hole lifetimes at the gold-donor level τ_n and τ_p in p-type samples can be defined by

$$\tau_n = \frac{1}{C_n^+ N_{Au}^+} = \frac{1}{C_n^+ N_A} \tag{7}$$

and

$$\tau_p = \frac{1}{C_p^0 N_{Au}^0} = \frac{1}{C_p^0 (N_{Au} - N_A)} \ , \tag{8}$$

where C_n^+ and C_p^0 represent the capture probabilities for electrons and holes at the positively charged and neutral gold-donor levels, respectively. The N_{Au}^+ is substituted by N_A using Eq. (4), and N_{Au}^0 is substituted by $(N_{Au} - N_A)$ using Eq. (3).

The reason that the minority-carrier trapping at the gold centers does not influence the steady-state excess-carrier lifetime is quite obvious for small injection cases. To be more specific, let us consider only the case of n-type gold-doped silicon: The gold-acceptor levels will act as recombination centers, while the gold-donor levels will act as hole-trap centers. The condition for a trap level is that the recombination rate at this level is negligible (compared to the recombination rate at the gold-acceptor levels). This means that the probabilities of electrons being captured by the gold-donor levels can be neglected. Therefore, we can set the electron recombination rate at the gold-donor levels to be zero, i.e.,

$$U_{tn} = 0 \ , \tag{9}$$

whereas for small injection the hole recombination rate at the gold-donor levels U_{tp} can be expressed by[6]

$$U_{tp} = C_p^0 (N_{Au}^0 \Delta p - p_{1t} \Delta N_{Au}^+) \ , \tag{10}$$

where p_{1t} denotes the hole concentration in the valence band when the donor level coincides with the Fermi level, and ΔN_{Au}^+ is the excess density of gold-donor levels being filled by the captured holes. For steady state, $U_{tp} = U_{tn} = 0$, since the capture of holes is exactly balanced by their emission. The steady-state electron and hole lifetimes τ_n and τ_p are given by

$$\tau_n = \frac{\Delta n}{(U_{cn} + U_{tn})} = \frac{\Delta n}{U_{cn}} \ , \tag{11}$$

$$\tau_p = \frac{\Delta p}{(U_{cp} + C_{tp})} = \frac{\Delta p}{U_{cp}} \ . \tag{12}$$

From Eqs. (11) and (12) we know that the steady-state excess-carrier lifetimes are only controlled by the recombination centers (i.e., the gold-acceptor levels). The only effect of these trap centers is their influence on the ac response times of the PME voltage, which will not be discussed in the present paper.

The rates of recombination of electrons and holes through recombination centers are equal in the steady-state case[6]

$$U_{cn} = \frac{\Delta n}{\tau_n} = U_{cp} = \frac{\Delta p}{\tau_p} \ . \tag{13}$$

If we define Γ as the ratio of excess electron and hole density, then from Eqs. (5)-(8) and (13) we find that

(a) For n-type material

$$\Gamma = \frac{\Delta n}{\Delta p} = \frac{\tau_n}{\tau_p} = \frac{C_p^- N_D}{C_n^0 (N_{Au} - N_D)} = \frac{N_D}{(N_{Au} - N_D)} \gamma_{1/2} \ , \tag{14}$$

where $\gamma_{1/2} = C_p^- / C_n^0$ is the ratio of hole- and electron-capture probabilities at gold-acceptor levels.

(b) For p-type material,

$$\Gamma = \frac{\Delta n}{\Delta p} = \frac{\tau_n}{\tau_p} = \frac{C_p^0 (N_{Au} - N_A)}{C_n^+ N_A} = \frac{(N_{Au} - N_A)}{N_A} \gamma_{-1/2} \ , \tag{15}$$

where $\gamma_{-1/2} = C_p^0 / C_n^+$ is the ratio of hole- and electron-capture probabilities at gold-donor levels.

From Eqs. (5)-(8) and (14)-(15), it is noted that one can easily control the lifetimes of excess carriers and the ratio of excess-carrier density simply by controlling the compensation ratio of N_{Au} and N_D for n-type samples, and N_{Au} and N_A for p-type cases.

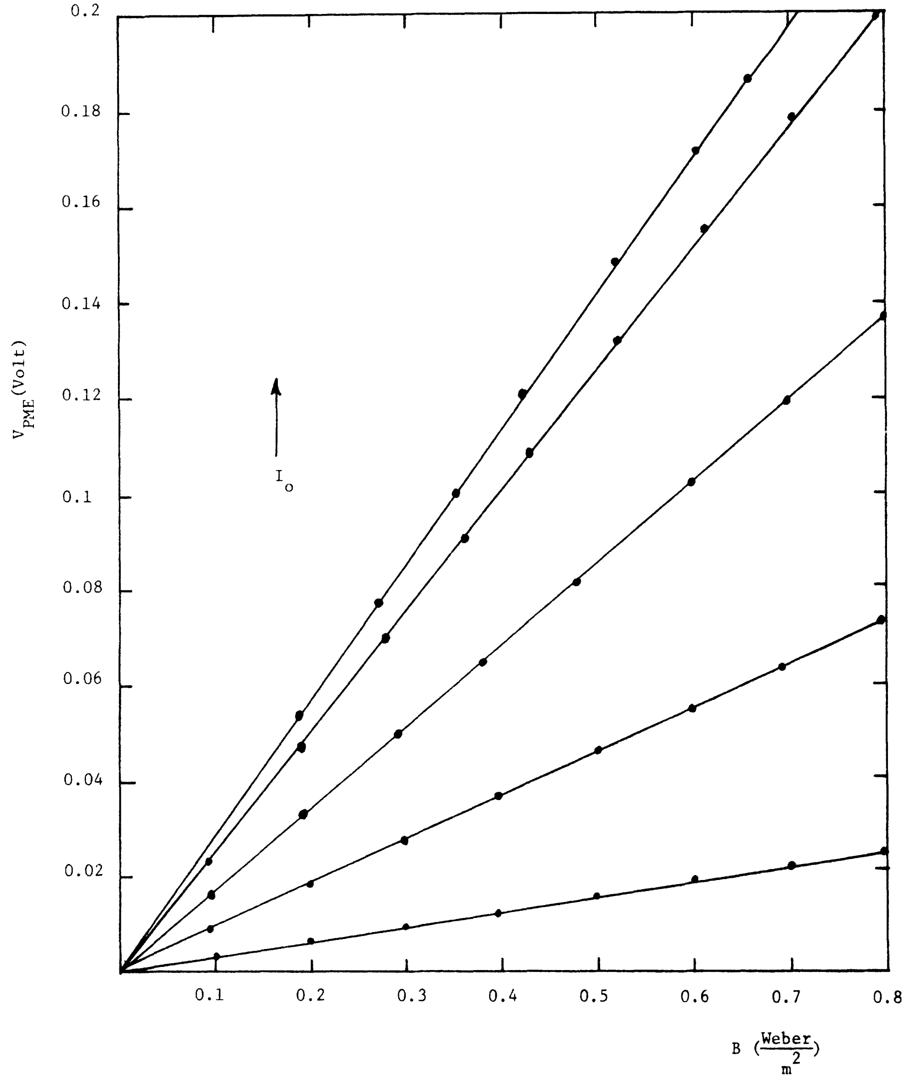

FIG. 1. The PME open-circuit voltage V_{PME} vs magnetic flux density B with light intensity I_0 as a parameter at $T = 300\,°K$ (for n-type sample).

B. PME and PC Effects

The results of Sec. IIA yield the relationship between the injected excess-carrier density for Au-doped silicon under small injection conditions. In this section, the results of Sec. IIA will be used in the derivation of the PME effect for Au-doped silicon. The electron- and hole-current density equations are given by[2]

$$J_{nx} = q\mu_n n\epsilon_x - \mu_n B J_{ny} \ , \tag{16}$$

$$J_{px} = q\mu_p p\epsilon_x + \mu_p B J_{py} \ , \tag{17}$$

$$J_{ny} = q\mu_n n\epsilon_y + qD_n \frac{d\Delta n}{dy} \ , \tag{18}$$

$$J_{py} = q\mu_p p\epsilon_y - qD_p \frac{d\Delta p}{dy} \ , \tag{19}$$

$$J_{ny} + J_{py} = 0 \ , \tag{20}$$

and the relation between Δn and Δp is given by Eqs. (14) and (15).

The continuity equation for electrons in the y direction (i.e., the direction of illumination) is given by

$$\frac{1}{q}\frac{d}{dy} J_{ny} - U_{cn} = 0 \ . \tag{21}$$

The boundary conditions at the illuminated and the dark surfaces of the sample are

$$[S_0 \Delta n - (1/q) J_{ny}]_{y=0} = Q \ , \tag{22}$$

$$[S_d \Delta n + (1/q) J_{ny}]_{y=d} = 0 \ , \tag{23}$$

where Q is the photon flux density. Solving Eqs. (16)-(20) and with $\Gamma = \Delta n/\Delta p$, we obtain the electron current density in the y direction

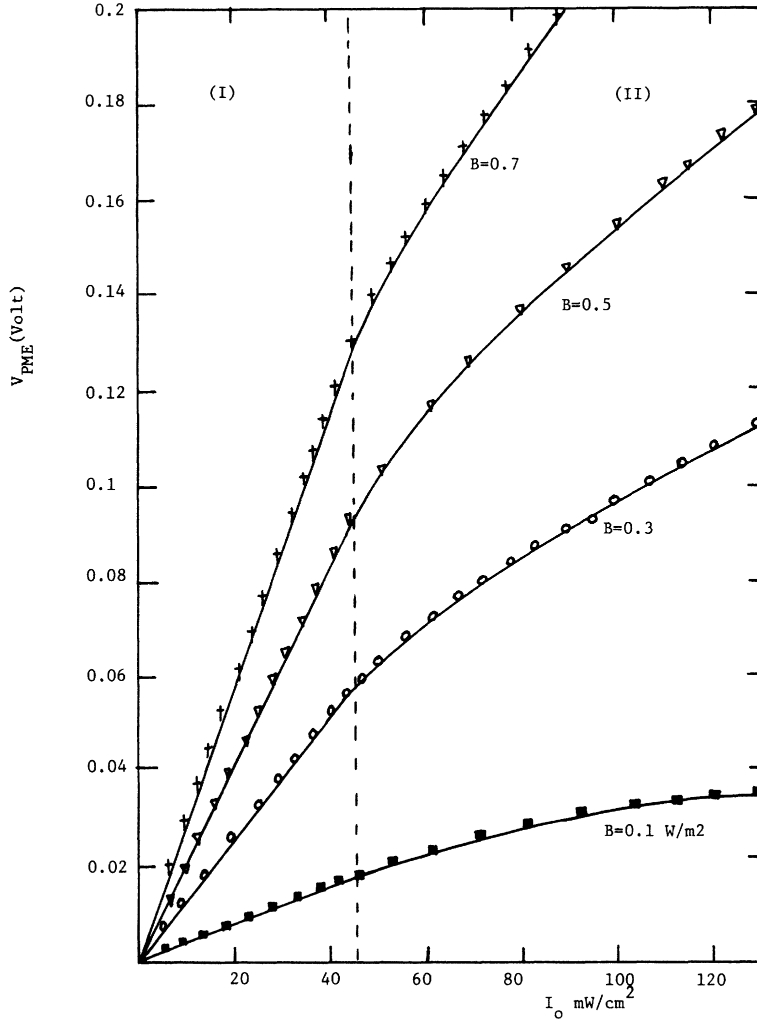

FIG. 2. The PME open-circuit voltage V_{PME} vs light intensity I_0 with magnetic flux density B as a parameter. Linear region (I), sublinear region (II) (for n-type sample), $T = 300\,°\mathrm{K}$.

$$J_{ny} \simeq \frac{qD_n(n_0\Gamma^{-1}+p_0)}{(n_0 b+p_0)}\frac{d\Delta n}{dy} = qD^*\frac{d\Delta n}{dy}\ , \tag{24}$$

where

$$D^* = \frac{D_n(n_0\Gamma^{-1}+p_0)}{(n_0 b+p_0)}$$

is the effective diffusion constant.

The PME short-circuit current per unit width (by setting $\epsilon_x = 0$) is given by

$$I_{\mathrm{PME}} = \int_0^d (J_{nx}+J_{px})\,dy = -B(1+b)\mu_p \int_0^d J_{ny}\,dy$$

or

$$I_{\mathrm{PME}} = qB(1+b)\mu_p D^*\Delta n_0\ , \tag{25}$$

where Δn_0 is the excess-carrier density at the illuminated surface. Δn_0 can be related to the incident photon flux density Q by solving the continuity equation (21) and using the boundary condition at $y = 0$. The result yields $\Delta n = \Delta n_0\, e^{-y/L^*}$ and

$$\Delta n_0 = L^*Q/(L^*S_0 + D^*)\ , \tag{26}$$

where $L^* = (D^*\tau_n)^{1/2}$ is the effective diffusion length.

The PME open-circuit voltage per unit length V_{PME} can be obtained from the relation[3]

$$V_{\mathrm{PME}} = I_{\mathrm{PME}}/G\ . \tag{27}$$

Substituting (25) into (27) we obtain

$$V_{\mathrm{PME}} = qB(1+b)\mu_p D^*\Delta n_0/G\ , \tag{28}$$

where $G = G_0 + \Delta G$, and G_0 is the dark conductance per unit width to length ratio. ΔG represents the photoconductance per unit width to length ratio which can be derived from

$$\Delta G = q\mu_p(b+\Gamma^{-1})\int_0^d \Delta n\,dy\ . \tag{29}$$

Substituting $\Delta n = \Delta n_0\, e^{-y/L^*}$ into Eq. (29) and using the boundary conditions that $\Delta n = \Delta n_0$ at $y = 0$ and $\Delta n = 0$ at $y = d$ in Eq. (29), we obtain

$$\Delta G = q(b+\Gamma^{-1})\mu_p L^*\Delta n_0\ . \tag{30}$$

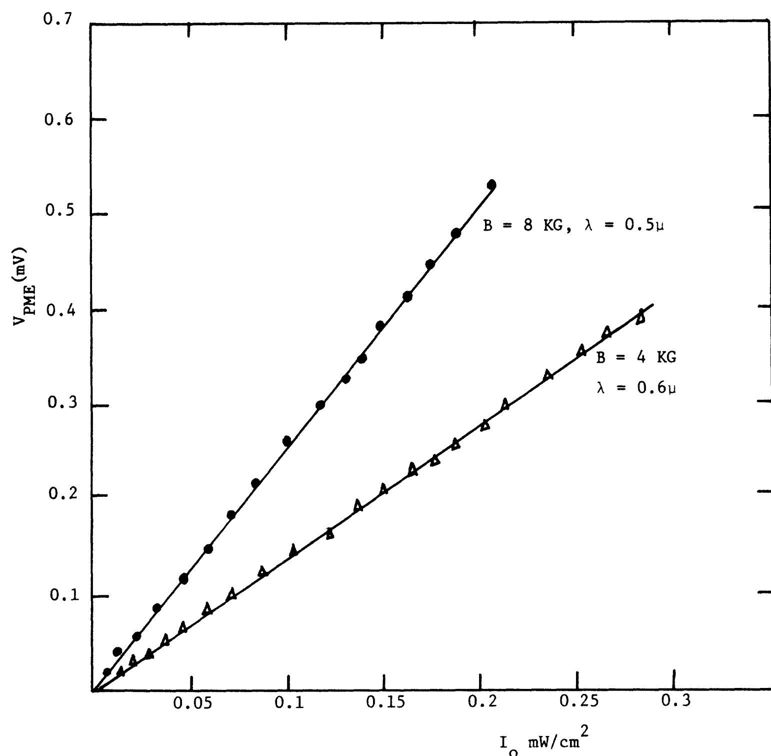

FIG. 3. V_{PME} vs I_0 for two different magnetic flux densities B and photon wavelength λ (for n-type sample), $T=300\,°K$.

The PME open-circuit voltage V_{PME} can now be expressed as a function of ΔG simply by eliminating Δn_0 from Eqs. (28) and (30). The result is

$$V_{PME}=B\left(\frac{b+1}{b+\Gamma^{-1}}\right)\left(\frac{n_0\Gamma^{-1}+p_0}{n_0b+p_0}\right)^{1/2}\left(\frac{D_n}{\tau_n}\right)^{1/2}\left(\frac{\Delta G}{G}\right) . \tag{31}$$

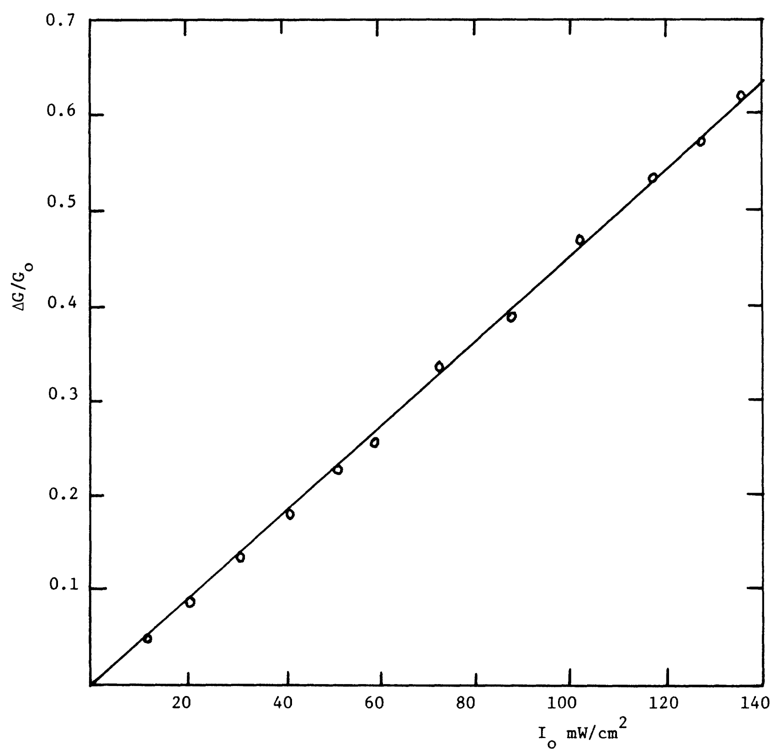

FIG. 4. Variation of the PC $\Delta G/G_0$ as a function of light intensity I_0 at $T=300\,°K$ (for n-type sample).

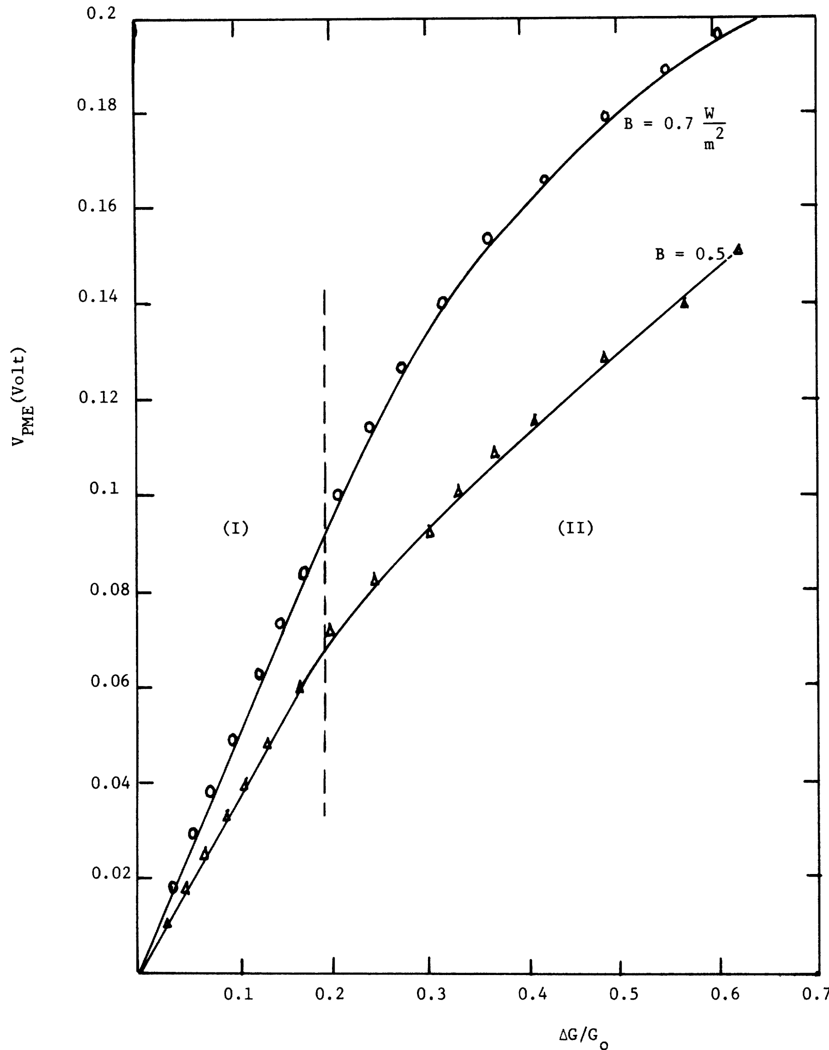

FIG. 5. Variation of the PME open-circuit voltage V_{PME} as a function of PC $\Delta G/G_0$ for two different magnetic flux densities B. Linear region (I) and sublinear region (II) for n-type sample, with $N_{\mathrm{Au}} \cong 5\times10^{16}$ cm^{-3} and $N_D = 10^{16}$ cm^{-3}, $T = 300$ °K.

Equation (31) predicts that for the small injection case (i.e., $\Delta G \ll G_0$), the PME open-circuit voltage V_{PME} should vary linearly with magnetic flux density B and the photoconductance ΔG (or light intensity).

Note that Eq. (31) provides a direct means for determining the electron and hole lifetimes as well as the capture probabilities from the concurrent measurements of the steady-state PME and PC effects as long as values of Γ are known. Equation (31) applies equally well for both p- and n-type samples. For n-type samples, Γ is determined from Eq. (14) and for p-type samples, Γ is determined by Eq. (15).

III. RESULTS AND ANALYSIS

An n-type silicon slice of 0.25-mm thickness, with phosphorus concentration $N_D = 10^{16}$ cm^{-3}, and a p-type silicon bar of 2-mm thickness with boron concentration $N_A = 10^{14}$ cm^{-3}, were used for gold diffusion. The wafers were treated by using ultrasonic cleaning in trichloroethylene (TCE) and rinsing in hydrofluoric acid (HF) followed by a thorough rinse in cold deionized water, before gold plating. Gold plating was achieved by immersing the samples in $\mathrm{AuCl_3}$ solution for about 24 h. The plating solution was prepared, as reported by Wilcox *et al.*,[7] by dissolving approximately 0.1 g $\mathrm{AuCl_3}$ in 1 liter 0.1M HCl + 0.5M HF solution. After gold plating, the wafers were placed in the furnace in an argon atmosphere for diffusion. The diffusion time was set for 24 h, and the diffusion temperature was 1200 °C. To prevent the gold atoms from precipitating, the wafers were quenched to room temperature after removing from the furnace. The samples were lapped and etched to a suitable size for electrical as well as photoelectric measurements. The final resistivity for the n-type sample was 4.2×10^3 Ω cm and for the p-type sample it was 1.9×10^3 Ω cm. To estimate the gold concentration

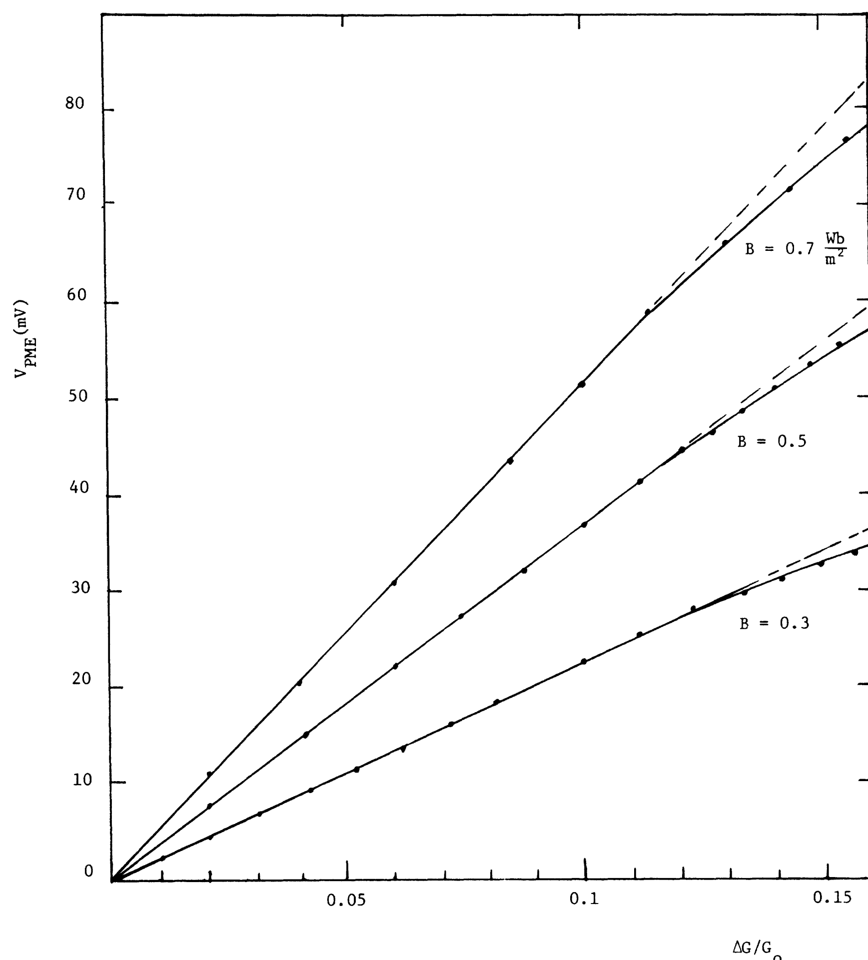

FIG. 6. Variation of the PME open-circuit voltage as a function of $\Delta G/G_0$ for various magnetic flux densities B for p-type sample, with $N_{Au} \cong 10^{16}$ cm^{-3}, $N_A = 10^{14}$ cm^{-3}, $T = 300$ °K.

from the resistivity and diffusion data, we used the theoretical curves calculated by Boltak *et al.*,[8] and the experimental data provided by Wilcox *et al.*[7] The estimated gold concentration for the n-type sample was found about 5×10^{16} cm^{-3} and 10^{16} cm^{-3} for the p-type sample. These measured gold concentrations are lower than the theoretical solid solubility of gold ($\sim 8\times10^{16}$ cm^{-3} at 1200 °C) calculated by Wackwitz[9] from the data of Struthers[10] and Collins.[11] However, the experimental results reported recently by Bullis and Strieter[9] and by Struthers[10] also indicate that the measured gold concentration is lower than the theoretical value. Note that the difference in gold concentration for both n-type and p-type samples for the present case may be due to the fact that our n-type sample was much thinner than that of the p-type sample during gold diffusion, which may have resulted in a higher gold concentration for the former.[12]

The sample dimensions for n type are $7\times5\times0.1$ mm^3 and $7\times5\times0.2$ mm^3 for the p-type sample. In order to satisfy the assumption (4) made in Sec. II, the front surface of the sample was chemically etched and the dark surface was sand blasted. The experimental setup and the measuring technique is identical to our previous report.[13]

The results of the PME and PC measurements are shown in Figs. 1–6. Figures 1–5 are the results for the n-type sample, and Fig. 6 is for the p-type sample. Similar dependence of V_{PME} on B, I_0 and ΔG on I_0, is observed for p-type samples and only V_{PME} vs $\Delta G/G_0$ is shown in Fig. 6 for the purpose of evaluation of carrier lifetimes.

Figure 1 shows the variation of V_{PME} vs B with light intensity I_0 as parameter. The results indicate that V_{PME} is directly proportional to B for various illumination intensities, which is in accord with the prediction of Eq. (31). Figure 2 shows the variation of V_{PME} as a function of light intensity with magnetic field B as parameter. The results indicate that at low illumination intensity a linear relation between V_{PME} and I_0 is obtained for various magnetic field strengths, and a sublinear region is observed for large illumination intensity. Figure 3 shows a linear relationship between V_{PME} and I_0 observed for two different wavelengths and magnetic

TABLE I. Recombination parameters in Au-doped silicon at 300 °K.

Sample		Bemski (Ref. 4)	Fairfield *et al.* (Ref. 3)	This paper
n type				
$N_{Au} \cong 5\times10^{16}$	C_n^0 (cm^3 sec^{-1})	5×10^{-9}	1.7×10^{-9}	1.8×10^{-9}
and	C_p^- (cm^3 sec^{-1})	1×10^{-8}	1.1×10^{-7}	1.3×10^{-7}
$N_D = 10^{16}$ cm^{-3}	τ_n (sec)	...	...	1.3×10^{-8}
	τ_p (sec)			7.8×10^{-10}
	L^* (cm)	...	...	1.0×10^{-4}
p type				
$N_{Au} \cong 10^{16}$	C_n^+ (cm^3 sec^{-1})	3.5×10^{-8}	6.3×10^{-8}	3.6×10^{-8}
and	C_p^0 (cm^3 sec^{-1})	$\geq 10^{-9}$	2.4×10^{-8}	1.4×10^{-8}
$N_A = 10^{14}$ cm^{-3}	τ_n (sec)	...	...	2.7×10^{-7}
	τ_p (sec)	...	...	7.3×10^{-7}
	L^* (cm)	...	...	22.1×10^{-4}

field strengths. The light intensity is rather weak when the monochromator is used for measurements. This can be seen by comparison between Fig. 2 (white light) and Fig. 3 (monochromatic light). Figure 4 demonstrates the linear relationship between $\Delta G/G_0$ vs I_0 which is again in accord with the prediction given by Eq. (30).

In order to compare the results with theoretical prediction of Eq. (31), we plot V_{PME} vs $\Delta G/G_0$ from Figs. 2 and 4. The results are shown in Fig. 5. Figure 5 demonstrates the variation of V_{PME} as a function of $\Delta G/G_0$ with B as a parameter for the n-type sample. The results indicate that for $\Delta G/G_0 < 0.2$ a linear relationship between V_{PME} vs $\Delta G/G_0$ is obtained, as is predicted by Eq. (31). For $\Delta G/G_0 > 0.2$, deviation from linearity was observed. The V_{PME} should become independent of $\Delta G/G_0$ at very high injection levels.[13] For the p-type sample, V_{PME} vs $\Delta G/G_0$ is shown in Fig. 6. One can again see that the linearity between V_{PME} vs $\Delta G/G_0$ is obtained for $\Delta G/G_0 \lesssim 0.12$.

In order to calculate the electron and hole lifetimes and the carrier capture probabilities at the gold levels, it is necessary to know the electron- and hole-capture rate ratios, $\gamma_{1/2}$ and $\gamma_{-1/2}$, at gold-acceptor and -donor levels, respectively. Using the data given by Fairfield and Gokehale[3] for gold-doped silicon, it is found that

$$\gamma_{1/2} = C_p^-/C_n^0 = 70, \quad \gamma_{-1/2} = C_p^0/C_n^+ = 0.38 .$$

Substituting the above values into Eqs. (14) and (15), one finds

$$\Gamma = 17.5 \text{ for } n\text{-type sample}$$

and

$$\Gamma = 38 \text{ for } p\text{-type sample.}$$

Using the above data and assuming $b = 2$ (the electron-hole mobility ratio), the electron lifetime is then computed from Eq. (31) and from the data in the linear region of Figs. 5 or 6. The result yields $\tau_n = 1.3\times10^{-8}$ sec for the n-type sample. The electron diffusion constant D_n for n-type sample used in the above calculation is 24.9 cm^2/sec and the hole-diffusion constant D_p for p-type sample is 8.8 cm^2/sec. These two constants are determined from the Hall-effect measurement (we have found $\mu_n = 960$ cm^2/V sec for n-type sample and $\mu_p = 340$ cm^2/V sec for p-type sample) and by using the Einstein relation $D_{n,p} = \mu_{n,p}(kT/q)$. In determining the scattering factor in the Hall coefficient, we have assumed that the LA mode lattice scattering is dominant (i.e., $r = 1.18$) and the scattering due to the gold impurity is negligible at room temperature. Other parameters such as τ_p, L^*, C_n^0, C_p^-, C_n^+, and C_p^0 are calculated subsequently by using Eqs. (5)–(8), (14), and (15). For comparison, the results are summarized in Table I, along with some available data in the literature.

IV. CONCLUSIONS

The PME and PC effects in gold-doped silicon have been studied at $T = 300$ °K. A linear relationship between PME open-circuit voltage vs magnetic field intensity, PC, and light intensity has been obtained in both n- and p-type samples under small injection conditions, which is in accord with the theoretical predictions of Eq. (31). This result indicates that the recombination and trapping mechanisms at room temperatures are quite different from those observed at low temperatures, as reported previously.[1,2]

A simple recombination model has been proposed to interpret the observed PME and PC effects in gold-doped silicon at room temperatures. The electron- and hole-capture probabilities at the gold-acceptor and -donor levels have been deduced from the PME and PC measurements, using the ratios of the electron-hole capture rate given by Fairfield *et al.*,[3] and the results are found in good agreement with those determined from other methods.

ACKNOWLEDGMENT

This research was supported in part by the Advanced Research Projects Agency, U.S. Department of Defense and monitored by the Air Force Cambridge Research Laboratories under Contract No. F 19628-68-C-0058.

[1]J. Agraz and S. S. Li, Phys. Rev. B 2, 4966 (1970).
[2]J. Agraz and S. S. Li, Phys. Rev. B 2, 1847 (1970).
[3]J. M. Fairfield and B. V. Gokehale, J. Solid State Electron. 8, 685 (1965).
[4]G. Bemski, Proc. IRE 46, 990 (1958).
[5]C. T. Sah, A. F. Tasch, Jr., and D. K. Schroder, Phys. Rev. Letters 19, 2 (1967); 19, 71 (1967).
[6]C. T. Sah and W. Shockley, Phys. Rev. 109, 1103 (1958).
[7]W. R. Wilcox, T. J. LaChapelle, and D. H. Forbes, J. Electrochem. Soc. 111, 1377 (1964).
[8]B. I. Boltaks, G. S. Kulikov, and R. Sh. Malkovitch, Fiz. Tverd. Tela 2, 181 (1960) [Sov. Phys. Solid State 2, 167 (1960)].
[9]Quoted in W. M. Bullis and F. J. Strieter, J. Appl. Phys. 39, 314 (1968).
[10]J. D. Struthers, J. Appl. Phys. 27, 1560 (1956).
[11]C. B. Collins, R. O. Carlson, and C. J. Gallagher, Phys. Rev. 105, 1168 (1957).
[12]G. J. Sprokel and J. M. Fairfield, J. Electrochem. Soc. 112, 200 (1965).
[13]S. S. Li, Phys. Rev. 188, 1246 (1969).

PHYSICAL REVIEW B VOLUME 4, NUMBER 2 15 JULY 1971

Electron-Phonon Scattering in Te-Doped GaSb at Low Temperatures

P. C. Sharma and G. S. Verma
Department of Physics, Banaras Hindu University, Varanasi-5, India
(Received 24 February 1971)

The reduction in the thermal conductivity of Te-doped GaSb samples at temperatures below the maximum conductivity temperature is explained in detail by considering the scattering of phonons by conduction electrons. The Ziman model has been used to fit the phonon-conductivity results on Te-doped GaSb samples with excess donor-electron concentrations in the range $1.6-1.8\times10^{17}$ cm^{-3}, where the impurity levels merge with the conduction band. At low concentrations of the order 1.6×10^{17} cm^{-3} the phonons are scattered by electrons in the ⟨000⟩ minima band and at concentrations exceeding 1×10^{18} cm^{-3} the phonons are scattered by electrons in the ⟨111⟩ minima band. At intermediate concentrations phonons are scattered by electrons in both the bands.

I. INTRODUCTION

Recently, Poujade and Albany[1] studied the role of electron-phonon scattering in the phonon conductivity of Te-doped GaSb at low temperatures in the range 5–100 °K. It was reported that at temperatures below the conductivity maximum at about 20 °K, the addition of donor impurities drastically reduces the thermal conductivity. Further, the increase in the thermal resistivity was directly proportional to the donor-electron concentration. The change in the conductivity due to doping was attributed to electron-phonon scattering. Poujade and Albany[1] explored several possibilities in explaining the electron-phonon interaction, but did not give any quantitative explanation of their results below the conductivity maximum, where electron-phonon scattering makes a major contribution towards thermal resistance.

There are two types of electron-phonon interaction in doped semiconductors at low temperatures depending upon the state of electrons. One interaction is important for electrons which are in semi-isolated impurity states which are found when the carrier concentrations are less than 10^{17} cm^{-3}. The other is important when the electrons are in the well-defined impurity band which occurs at higher concentrations. In materials with sufficiently high donor-electron concentration the impurity levels merge with the conduction band. The conduction electrons for such materials form a degenerate assemblage. Ziman[2] calculated the cross section for the scattering of phonons by electrons in a conduction band. The cross section depends upon the number of occupied donor electrons. He gave an expression for the relaxation rate of the electron-phonon scattering to satisfy the requirements that energy and momentum are conserved in the phonon-electron scattering. It is shown in the present work that quantitative explanation of the decrease in the values of phonon conductivity with doping, as well as its temperature dependence, can be obtained on the basis of Ziman's scattering for all the samples of Te-doped GaSb with donor-electron concentrations greater than 10^{17} cm^{-3}. One of the interesting conclusions of the present work is that at low donor-electron concentration of the order 1.6×10^{17} cm^{-3} the phonons are scattered by electrons in the ⟨000⟩ minima band. At concentrations exceeding 1×10^{18} cm^{-3}, the phonons are scattered by electrons in the ⟨111⟩ minima band. At intermediate concentrations phonons are scattered by the electrons in both the bands, and one can predict, from the study of the density-of-states effective mass, the number of electrons in ⟨000⟩ and ⟨111⟩ minima bands.